A NEW METHOD FOR CALCULATING LUMINOUS FLUX USING HIGH DYNAMIC RANGE IMAGING AND ITS APPLICATIONS

BY

Reid M. Poling

Submitted to the graduate degree program in Architectural Engineering and the Graduate Faculty of the University of Kansas in partial fulfillment of the requirements for the degree of Master of Science.

____

Chairperson Dr. Hongyi Cai

____

Dr. Brian Rock

____

Dr. Mario Medina

Date Defended: 05/03/2018

The Thesis Committee for Reid Poling

certifies that this is the approved version of the following thesis:

A NEW METHOD FOR CALCULATING LUMINOUS FLUX USING HIGH DYNAMIC RANGE IMAGING AND ITS APPLICATIONS

____

Chairperson Dr. Hongyi Cai

Date approved:

ABSTRACT

High Dynamic Range (HDR) photography is a camera-aided tool for measuring luminance and glare. This study explored a method of using HDR images to estimate luminous flux (in units of lumens) contributed from light sources and surfaces visible to the camera lens. The goal was to validate this camera-aided method for remote measurement of luminous flux and check its applications in a real lit environment. A pilot study was first conducted in the illumination laboratory (2400 LEEP2) to explore the idea and develop a series of equations, followed by a laboratory experiment using an integrating sphere to validate the method with an error of 6.2%. Next, the new method was used to estimate luminous flux in a real luminous environment. In a prior study, a series of HDR images were taken in an office space under fluorescent and LED lighting with varying levels of lighting control offered to a total of 30 participants. The wattage consumption of the lighting systems under each test scenario was also recorded. In this study, those HDR images were calibrated and analyzed to obtain per-pixel luminance data. Equations were then used to calculate lumens attributed from all surfaces and light sources in the office visible to the camera lens under different lighting conditions. The so calculated luminous flux obtained from the HDR images of different lighting settings was then compared with the associated wattage of the corresponding lighting condition. It was found that luminous flux and electrical energy were closely corelated. Luminous flux increased or decreased in the same way as wattage. This study proved that the new method for calculating luminous flux using high dynamic range imaging method is valid and useful for lighting practice and research.

ACKNOWLEDGEMENTS

Many thanks to Dr. Hongyi Cai, chairperson of my committee, for his many contributions to my academic career. He offered countless hours of help and guidance during this study as well as other coursework throughout my college years. This paper would not be possible without his help.

I must also thank my committee members, Dr. Brian Rock and Dr. Mario Medina, who have helped me in my studies.

Thanks also to Faran Mahlab, Hankun Li, Habib Arjmand Mazidi, and Simon Diederich for helping at various times with my pilot and verification experiments and tests.

I should also thank Linjie Li, whose previous work on his own Master's thesis provided the data and photographs used for a large part of my own thesis.

I also need to thank my family and friends for giving me support throughout my academic career.

TABLE OF CONTENTS

NOMENCLATURE

Φ : Luminous Flux, in *lumens*

Ω : Solid angle of the surface, unitless

A : True area of a surface/object

A_{app} : Apparent area of the surface, in m^2

L : The luminance of the surface, in cd/m^2

I : Luminous intensity, in *cd*

θ : Incidence angle

φ : Tilt angle

r_1 : Distance from camera lens to object

r_2 : Distance from focal point to image pixel

f : Focal length of camera lens, 4.5*mm*

d : Distance from center pixel of imaging sensor to center pixel of area of interest, in *mm*

X : X coordinate (left-right) of point of interest in the field. Negative to the left, with the camera focal point at the center

Y : Y coordinate (front-back) of point of interest in the field. Negative to the rear, with the camera focal point at the center

Z : Z coordinate (up-down) of point of interest in the field. Negative is down, with the camera focal point at the center.

LIST OF FIGURES

LIST OF TABLES

CHAPTER 1 INTRODUCTION

1.1 BACKGROUND

1.1.1 LUMINOUS FLUX

Luminous flux is the measurement of light output in lumens. Luminous flux is directionally dependent, meaning that only a fraction of the total lumens coming from a light source or surface reflectance is emitted in any one direction. As a result, the luminous flux visible to the eyes of a space user at a specific viewing direction will only be a small portion of the total lumen output of the lighting system in that space. In lighting practice, it is important to know the amount of light exposure (in lumens) in interested viewing directions of space occupants for providing high quality and healthy lighting solutions.

When lighting manufacturers release a new luminaire, the number of lumens that luminaire outputs are listed in the specification sheet and is an important aspect in designing the lighting of a space. The listed lumen value refers to the total number of lumens that the luminaire emits in all directions. An integrating sphere is used by manufacturers to measure the total luminous flux in any direction (360 degrees). Often manufacturers also provide zonal lumens of that luminaire in interested directional zones (e.g., 0 – 10 degree) for the benefit of lighting design.

Integrating spheres are the accurate and reliable way to measure total luminous flux of a lighting fixture. A fixture is placed in the center of the sphere, which has a highly diffusive reflective white interior surface, wherein sensors are used to measure the total lumens that the fixture emits. However, this laboratory method cannot be used for measuring luminous flux output in a real luminous environment in practice. Directional luminous flux information in rooms, as is the context of this study, cannot be found using integrating spheres. In a room, light received at a point comes from all objects and surfaces visible to that point. Moreover, the numbers of directional luminous flux will be affected by the light reflection of a wide variety of surfaces within a room and human-light interactions in the real luminous environment.

On the other hand, lumens are directionally dependent, and a space occupant can only see objects and surfaces within his/her field of view, which is not 360 degrees. Lighting professionals often need to estimate how much luminous flux actually arrives at the eyes of the space users in a specific viewing direction at a specific viewing point, for better lighting layout and high quality and healthy lighting design. Unfortunately, as of today, there is no fast, accurate, and reliable way to measure the luminous flux that reaches the eyes of a space user at any viewing direction. The number will be only a very small portion of the total light emitted in a space in all directions. In lighting practice, instead, light meters are used to measure other lighting metrics, such as horizontal and vertical light levels in illuminance, or luminance of any interested surfaces at typical viewing directions of space users.

In lighting practice, it is useful to determine what part of the space contributes how much light. Luminous flux is related to luminous exitance, which is the amount of light leaving a surface. Luminous flux is also related to the electrical energy usage for lighting the space. Theoretically, as lumens increase, so should the electrical energy consumption.

This study will explore a new method of measuring directional luminous flux in a real luminous environment using High Dynamic Range photography. The lumens contributed from objects and surfaces visible to the camera lens (eyes of the space users) will be measured in a different form than what is found in integrating spheres.

1.1.2 HIGH DYNAMIC RANGE (HDR) PHOTOGRAPHY

High Dynamic Range images are high resolution photographs that greatly resemble the wide range of light and color of the scene being captured by the camera. These images are exceedingly close to what the human eye can see.

The process of creating an HDR image involves several steps. The camera used in this study is a Canon T2i digital camera with a 4.5mm fisheye lens, though a standard lens can be used if desired. The camera is set in the desired position, and then a series of 18 standard low dynamic range (LDR) images were taken. Low dynamic range images are a single image taken at a single shutter speed, much like the typical images taken with most readily-available cameras. Each of the LDR images necessary to create an HDR image are taken with different shutter speeds, from slow to long shutter speeds. These produce images that are overexposed, which show little more than an almost white image, or underexposed dark images where very little is distinguishable, and everything in between. Figure 1 shows some overexposed and underexposed LDR images used in an HDR image. Combining all 18 LDR images using the software Photosphere returns an HDR image that represents a remarkably true image of the space as in Figure 2.

(a) Overexposed Low Dynamic Range image with low shutter speed

(b) Underexposed Low Dynamic Range image with high shutter speed

Figure 1: Low Dynamic Range (LDR) images with different exposures used in creating a High Dynamic Range (HDR) image

Figure 2: A finalized HDR image of a test office space

For lighting measurement, HDR images are able to return the luminance of different surfaces. Luminance is a measure of the brightness of a point and is measured in cd/m^2. Luminance is useful in determining the glare potential of a lit environment, and where that glare is most likely to occur. Several software packages are available that take the RGB color value of each pixel in an HDR image to determine the luminance of the pixel. The HDR image needs to be calibrated to show a truly accurate representation of the luminance in the actual environment. A hand-held luminance meter is typically used to measure the luminance of a set point of a reference target in the field which is then used to calibrate the image based on the luminance of the same point in the HDR image. Vignetting corrections are used to correct the light drop off from the image center to peripheral area due to the imperfection of the camera lens. Photogrammetrical calibrations are also necessary for fisheye lenses to account for any distortions the lens causes to the image.

For this study, the software HDRscope (Kumaragurubaran, Inanici, 2012) is used as the main tool for measuring the luminance of an HDR image. Another software, Photosphere (Ward) is also used for control. The luminance is a key element in calculating the luminous flux.

1.2 GOAL AND OBJECTIVES

The goal of this research was to develop and validate the new method of using HDR images to estimate luminous flux (in lumens) contributed from light sources and surfaces that are visible to the camera lens (or eyes of the space users) mounted at a specific view point. To realize that goal, three objectives were achieved in this study as follows:

(a) Explore and develop the method in a pilot study conducted in the illumination laboratory in 2400 LEEP2.

(b) Validate this camera-aided method for remote measurement of luminous flux in a well-controlled laboratory experiment conducted using an integrating sphere.

(c) Check its applications in a real lit environment, in an office space under fluorescent and LED lighting with varying levels of access to continuous dimming control offered to a total of 30 participants.

.

Luminance of a surface or object, its solid angle, and corresponding apparent area are the three values needed for calculating lumens, as will be discussed later in Chapter 3. Per-pixel luminance was found from the HDR images in the HDRscope software with calibrations using Photosphere. A pilot test was conducted in the illumination laboratory to determine how to find solid angles and apparent areas from the pixel coordinates available in an HDR image. Another test was carried out in a well-controlled laboratory environment in the dark room (1152 Learned Hall) with an integrating sphere to determine the validity and accuracy of the procedure in accurately calculating luminous flux.

The final part of this study was using the aforementioned method of calculating lumens on a series of HDR images in an office environment. Four sets (fluorescent and LED with and without access to continuous dimming control) of 30 HDR images of the office luminous environment were analyzed using the determined procedure. Each set of 30 images was set in a different lighting scenario including: LED lights with and without access to continuous dimming control, and fluorescent lights with and without access to continuous dimming control. Each of the 30 images in a set was taken for a different user from a previous office ergonomics study (Li, 2013). Each of these images returned a lumen value and were compared with the electrical energy usage as well as the lumen value for the same test subject under different lighting scenarios.

Calculating the luminous flux in this way can be useful for future research as well. In general, HDR images are powerful tools for lighting measurement, but are currently limited in what they can measure. This methodology seeks to expand the capability of HDR imaging in light measurement to record luminous flux.

CHAPTER 2 LITERATURE REVIEW

2.1 LUMINOUS FLUX AND LUMINANCE

Luminous flux has been understood for some time, as has luminance. Luminous flux is typically considered the total light output of a luminaire or lamp, as measured by integrating spheres. The theory behind integrating spheres has been well established, as companies have developed to manufacture and sell integrating spheres for wide spread use by lighting manufacturers. Scholarly articles such as Wolpert's 1983 paper on "Unraveling the Mystery of Integrating Spheres" discusses the function and theory of integrating spheres (Wolpert, 1983). Further explanations on integrating spheres can be found easily from manufacturers, such as Labsphere's technical guides to its products. Because these tools are trusted instruments in the field of lighting measurement, especially for luminous flux, an integrating sphere will be used in conjunction with HDR imaging to validate the method developed for this paper.

For developing the equation of calculating luminous flux from the information in an HDR image, it is also necessary to understand the relationship between luminous flux and luminance, the primary value determined from HDR images. Put simply, the luminous flux is the product of luminance, apparent area, and solid angle (Levin, 1968).

This simple mathematical relationship between two light metrics has been used in a few other studies. Fung and Chang developed a method of using a luminance meter to estimate the luminous flux of a backlight meter (Fung & Chang, 2007). This method is the most like that developed for this paper but varies in some major ways. First of all, they use a standard hand-held luminance spot meter instead of HDR imaging. Furthermore, they use their method to measure total lumen output of a backlight fixture, comparing the lumen output to that found in an integrating sphere. They also use a different definition of solid angle. As will be mentioned in Chapter 3 of this paper, the solid angle used for this paper is a function of apparent area and distance, whereas Fung and Chang use the incidence angle of the meter aimed at the light. Their method would be more difficult to apply to the context of this experiment. As different surfaces throughout a room vary in relation to the camera, the incident angles would become tedious and difficult to calculate. Using apparent area and an estimated distance to the surface in question is more appropriate for this experiment. Brazel and Krochmann (1986) also developed a method in estimating a lamp's luminous flux by measuring the luminance. However, since this paper looks at measuring only a fraction of all lumens in a room, the methods of Brazel and Krochmann or Fung and Chang are not applicable to this application. Both of these previous papers essentially develop a replacement for an integrating sphere. The HDR method will only measure the lumens output in a certain direction, and from multiple different surfaces and objects in a room.

2.2 HIGH DYNAMIC RANGE PHOTOGRAPHY

Many papers have been published regarding High Dynamic Range photography and measuring luminance. High Dynamic Range images are able to capture the luminance of pixel points, representing a much truer representation of the actual brightness of a surface or object than a handheld meter like a Minolta LS-100 Luminance

Meter. Hand-held meters use an average of the visible area to measure luminance, while HDR images can show more specific luminance values of individual points. HDR images also have high resolution and can show changes in luminance over changes in geometry as well, thus essentially producing results very similar to human vision. It has also been proven that HDR images are anywhere from 1.5% to 10.1% accurate in measuring luminance, which proves the method is a reliable tool (Cai, et al., 2017).

The reliability of HDR images to give accurate measurements of luminance has served as the basis for many different software packages that measure and analyze the luminance data available in HDR images. Radiance typically acts as the base code for many of these programs, which converts the RGB color values of pixels into luminance values. Programs like Photosphere, Evalglare, and HDRscope have all been developed to display this given luminance value, as well as analyze luminance for glare potential. This paper uses HDRscope as the tool for measuring luminance.

HDRscope is the result of extensive programming and development detailed in papers by Kumaragurubaran and Inanici (2012; 2013). HDRscope differs from other software in its ability to show statistical results of luminance over varying areas of an image. It also aims to be user friendly and provide multiple ways to select and measure areas in an image. Programs like Photosphere are limited in only allowing strict rectangular areas or individual pixels to be analyzed. HDRscope has circular and polygon selection tools available, thus making it easier to study oddly shaped areas, such as triangles, irregular polygons, and circles. As will be discussed in Chapter 3, in discussing the methodology of this experiment, almost all areas in the room needed the polygonal area selection tool that only HDRscope is able to provide.

Very little has been done with HDR imaging outside of luminance and glare measurement. Moeck and Anaokar (2006) developed a method of measuring illuminance using HDR images. Illuminance is the amount of light arriving at an individual point. Although the type of metric they are trying to measure is different from luminous flux, Moeck and Anaokar have shared the overarching goal of this paper of increasing the number of lighting values that an HDR image can measure.

2.3 PHOTOGRAMMETRY

A key factor in the procedure this paper outlines is estimating the physical distance from the camera lens to any particular point in the room. This distance is needed for estimating the apparent area and can even be used to estimate the solid angle. One of the goals of this experiment is to only use the image to estimate the number of lumens. A technique developed by Cai (2012) allows the physical, in-field coordinates of any point in an image to be determined based on image pixel location. This can be done with minor field measurements.

In order to find the in-field coordinates of any point in an image, the various planes need to be defined. The plane on which any surface lies is found by measuring the X,Y, and Z coordinates of at least three points on that plane. Using these reference points, their image pixel coordinates, and any rotation of the plane or camera, yields an equation for finding the X, Y, and Z coordinates of any other point on that plane (Cai, 2012). This method is an important step in calculating the apparent areas, as outlined in Chapter 3 of this paper.

CHAPTER 3 METHODOLOGY

3.1 MATHEMATICAL BASIS

3.1.1 LUMINOUS FLUX

Luminous flux (Φ) can be defined as a function of lighting intensity in any given direction. The mathematical representation of luminous flux is demonstrated as:

$$\Phi = \int_0^{\Omega} I(\theta, \varphi) d\Omega \quad (1)$$

The intensity ($I(\theta, \varphi)$) in any given direction is defined as:

$$I(\theta, \varphi) = L * A_{app} \quad (2)$$

Substituting equation 2 into equation 1 gives:

$$\Phi = \int_0^{\Omega} (L * A_{app}) d\Omega \quad (3)$$

Which continues to simplify to:

$$\Phi = L * A_{app} * \Omega \quad (4)$$

The light output from any object or surface is simply the product of luminance, apparent area, and solid angle.

3.1.2 APPARENT AREA

Luminance will be calculated from the HDR image using HDRscope. It is therefore necessary to calculate the apparent area and solid angle for the object in question. Apparent area is the projected area of an object. In other words, this is the area of the object that can be seen from a certain perspective. As incidence angles change, so does the area that is visible. The relationship between area and incidence angle is defined as:

$$A_{app} = A * \cos(\theta) \quad (5)$$

Incidence angle (θ) is the angle between the line of sight and the normal vector to the surface. The area, A, is the true area of the object.

Apparent area and solid angle are also related. This relationship is stated as:

$$A_{app} = \Omega * {r_1}^2 \quad (6)$$

The distance, r_1, of equation 6 is the distance from the camera lens to the item. This definition of apparent area is the most conducive to the method outlined in this paper, as both the solid angle and distance, r_1, can be estimated from just the image, with little field measurements necessary.

3.1.3 SOLID ANGLE

Solid angle is a three-dimensional representation of an angle as determined in the context of a sphere. Figure 3 exhibits a visual representation of a solid angle.

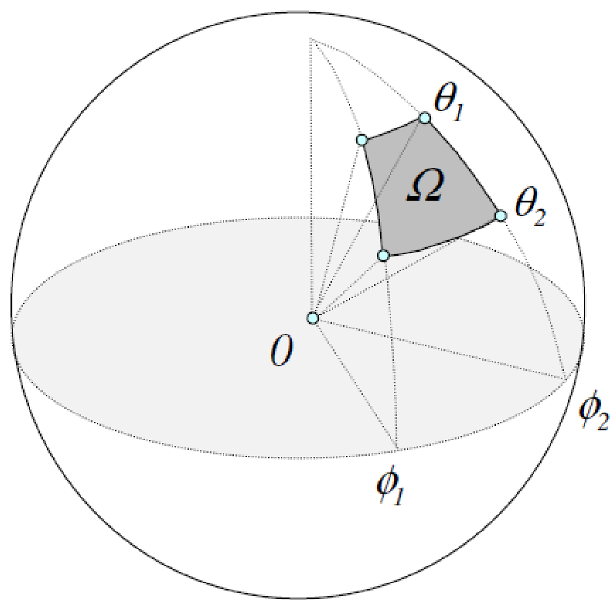

Figure 3: 3-Dimensional representation of solid angle (www.et.byu.edu)

The solid angle demonstrated in Figure 3 can be calculated using either the set of angles θ and ϕ, or the projected area and radius of the sphere. The relationship between area and radius is the most reasonable in the context of photographs, as was discovered in the pilot study. This relationship is defined as:

$$\Omega = \frac{A}{r^2} \tag{7}$$

These equations for solid angle and apparent area are used in conjunction with the luminance value found from HDRscope to calculate the lumens output from a point towards the camera lens. The process of calculating apparent area and solid angle from an image were established in a pilot study.

3.2 PILOT STUDY

3.2.1 INTRODUCTION AND SET UP

The pilot study served as the first test of calculating lumens using Equation 4. Instead of calculating the lumens from every surface in the image, this test was limited to four pieces of white, 8.5”x11” copier paper. The area of each paper is set, which helped in finding the apparent area and solid angle, which were the main focus of this test. The goal was to find these two values with as little field measurement as possible, instead, trying to find these values from just the information in the HDR image.

This test was carried out in the 715-sq. ft. Henderson Engineers Illumination Laboratory in 2400 LEEP2. The lab consists of three main areas: a test area, teaching area, and a student desk/work area. The testing section on the south side of the lab has some LED fixtures in half of the space and is able to be surrounded by black curtains.

The desk and teaching area have linear fluorescent pendant lights. A large television presentation screen is on the north side of the room, along with a window overlooking an indoor atrium. All lights except the LED fixtures in the test area were on for the experiment. Two of the four pieces of paper used for the test were placed on the large table in the middle of the teaching space, with the others being placed on the West and South walls.

An X, Y, Z coordinate axis was established in the room with the focal point of the camera being the center of the coordinate system. Cai's photogrammetry method (2012) was used to estimate the physical distance from the camera to the lens. Because photogrammetry needs X, Y, and Z coordinates for at least three reference points on each plane, these reference points were established for the three surfaces on which the papers were placed, and the coordinates were measured in the room using a laser distance meter. The distance from the camera lens to the center of each paper was also measured to compare with the result from the photogrammetry calculation. With the distances to each reference point and the associated pixel location of each reference point in the HDR image, the photogrammetry equation can estimate the actual distance to any point on the same plane of the reference points. The layout of the room, reference points, and papers are shown and labeled in Figure 4.

Figure 4: Pilot test layout, test paper locations (P1, etc.), and reference point (R1, etc.) locations used in pilot study

The Canon T2i camera with fisheye lens was set at a height of 4.16 ft and aimed at the center of P1. Eighteen LDR images were taken and then compiled using Photosphere into an HDR image. A Minolta LS-100 Luminance hand meter was used to measure the luminance of the third from the left bottom gray square on the color checker card seen on the table, which was used to calibrate the luminance of the HDR image.

With the four papers set up, the HDR image taken, and the necessary field measurements for the reference points taken, the luminance, apparent area, and solid angle could be found. Luminance was found using HDRscope. Apparent area and solid angle were each calculated two separate ways. One approach used the field measurements, and the other used photogrammetry and pixel locations and areas.

3.2.2 APPARENT AREA CALCULATION

The apparent area could be found using either of Equations 5 and 6. These two equations correlated to two separate methods tested in this pilot study. The two methods were:

Method 1: $A_{app} = A * \cos(\theta)$

Method 2: $A_{app} = \Omega * r_1^2$

Method 1 consisted of using the known area of 8.5"x11" copier paper as the primary area, *A*. The incidence angle for each paper was found using field geometry, as shown in Figure 5 below.

Horizontal Papers:

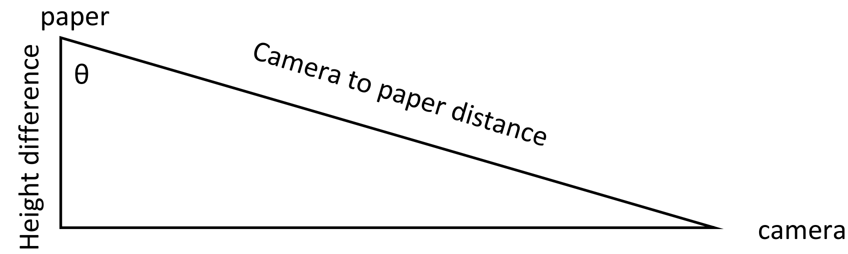

Vertical Papers:

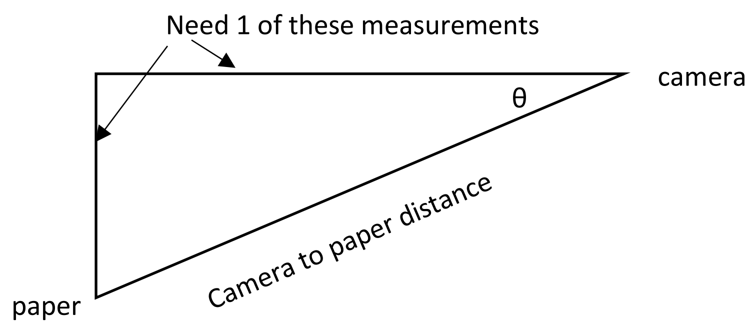

Figure 5: Incidence angles for horizontal and vertical targets

Using the incident angles and area of a sheet of paper, the apparent area of each of the four sheets of paper was found. These are tabulated in Table 1.

Table 1: Apparent Areas Using Field Measurements (Method 1)

Apparent Areas			
Paper #	θ	A (in^2)	A_{app} (m^2)
1	59.710	93.50	0.030
2	73.120	93.50	0.018
3	53.500	93.50	0.036
4	20.360	93.50	0.057

Method 2 required the solid angle and the photogrammetry calculations. Method 2 was a way to find apparent area without needing field measurements as in Method 1, and only used the data available in an HDR image. This is the method used in the final office lighting tests of this paper.

Equation 6 requires a distance, r_1. This distance was that from the camera lens to the object, which was each piece of paper in this case. Photogrammetry returns the X, Y, and Z coordinates of the point of interest in relation to the camera, so r_1 was defined as:

$$r_1 = \sqrt{X^2 + Y^2 + Z^2} \tag{8}$$

The results of the photogrammetry calculations for r_1 are given in Table 2 as well as the field measured distances for comparison. The results are very similar, so photogrammetry is a reliable tool for finding distances from HDR images.

Table 2: Photogrammetry Results for In-Field Distances

Target Point	notes	X (m)	Y (m)	Z (m)	Distance to lens (m)	Distance to lens (ft)	Actual Measured Distance to lens (ft)
paper 3	center of paper	2.293	1.341	-2.333	3.535	11.598	12.140
paper 4	center of paper	0.132	6.156	0.043	6.157	20.201	20.960
paper 1	center of paper	0.244	1.046	-0.525	1.196	3.922	3.430
Paper 2	center of paper	-0.300	1.920	-0.524	2.013	6.603	5.960

Using the distance found in Table 2 as the value r_1, Method 2 then required the solid angle. The solid angle could be found using only the HDR image as well, and will be detailed as the second method of finding solid angle in Section 3.2.3. The solid angles for each paper are combined with the distances from Table 2 into Equation 6. Table 3 displays the solid angle for each paper that was used, and the corresponding apparent area. The apparent area from Method 1 is also included for comparison.

Table 3: Apparent Areas from HDR Image Pixel Coordinates (Method 2)

Target Point	notes	Method 2 Paper Solid Angle	Method 2 Apparent Area (m^2)	Method 1 Apparent Area (m^2)
paper 3	center of paper	0.0021	0.0262	0.0359
paper 4	center of paper	0.0010	0.0379	0.0566
paper 1	center of paper	0.0254	0.0363	0.0304
Paper 2	center of paper	0.0034	0.0138	0.0175

3.2.3 SOLID ANGLE CALCULATION

Similar to the apparent area, the solid angle was found with two different processes. Both methods used Equation 7. The difference between each method was the area, *A*, and distance, *r*, that was used. The two methods for solid angles were:

Method 1: $\frac{A_{app}}{{r_1}^2}$

Method 2: $\frac{A_{imaging\ sensor}}{{r_2}^2}$

Method 1 used the field measured values. The apparent area is that which was calculated using Method 1 for apparent areas. The camera to paper distance was measured in the field using a laser distance meter. These solid angles are tabulated in Table 4.

Table 4: Solid Angles Using Field Measurements (Method 1)

Solid Angles Using Measured Geometry			
Paper #	Distance to Paper (ft)	A_{app} (ft^2)	Solid Angle (Ω)
1	3.43	0.33	0.0278
2	5.96	0.19	0.0053
3	12.14	0.39	0.0026
4	20.96	0.61	0.0014

Method 2 was a more involved process but maintained the benefit of only using the HDR image without any field measurements necessary. The area used for this method was the area that the paper occupied on the imaging sensor of the camera. The imaging sensor for the Canon T2i camera is 14.9 mm x 22.3 mm, with a corresponding pixel layout of 3456 x 5184. With this known, it was easy to find the physical width of each pixel on the imaging sensor. The pixel coordinates of the corners of each piece of paper could then be used to find the number of pixels contained in the image of the paper, and thus the area of the paper on the imaging sensor. This was used as the value, *A*, in Equation 7.

The distance, r_2, is the distance from the focal point of the camera to the center pixel of the area. The focal length is 4.5 mm, which is the distance from the focal point to the center pixel of the imaging sensor. Finding r_2 was then a simple triangular relationship between the focal point, center pixel, and center pixel of the paper, as shown in Figure 6.

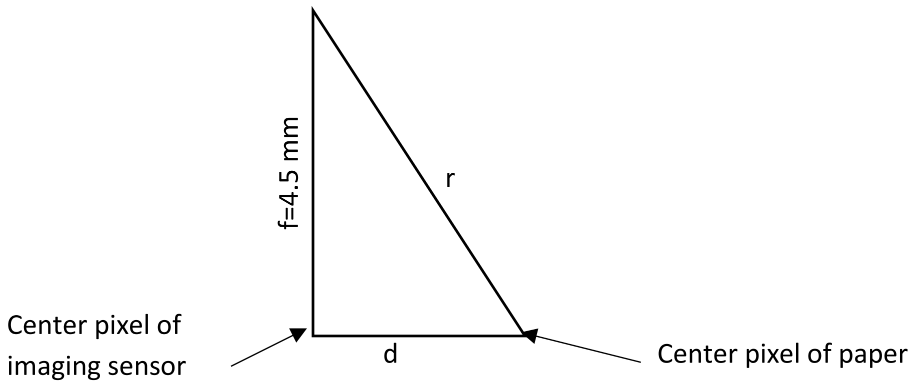

Figure 6: Distance, *r*, for solid angle calculation from HDR image

The pixel coordinates for the center pixel of the imaging sensor, and the center pixel for the paper were found easily in HDRscope. The distance between the two pixels was the value, *d*, in Figure 6. With the focal length and *d* known, r_2 could be found. This was then used in Equation 7 along with the area of the paper on the imaging sensor to find the solid angle. This solid angle was consequently used as the solid angle in Method 2 for calculating apparent area, as detailed in the previous section. Table 5 shows the results for solid angles found with Method 2.

Table 5: Solid Angles Using HDR Pixel Coordinates (Method 2)

Paper #	Area on Image Sensor (mm^2)	Center Pixel to Area Center (d) (mm)	Radius (r) for Solid Angle (mm)	Solid Angle (Ω)
1	0.5146	0.1504	4.5025	0.0254
2	0.0798	1.7066	4.8127	0.0034
3	0.0677	3.3623	5.6174	0.0021
4	0.0249	1.9115	4.8892	0.0010

3.2.4 PILOT STUDY RESULTS

This pilot study served as a way to test methods for calculating luminous flux using only an image. Method 2 for both apparent area and solid angle achieved this goal. Substituting apparent area, solid angle, and luminance for each paper into Equation 4 returned the luminous flux from each paper. Method 2 (image only) was treated as the test value, while Method 1 (field measurements) acted as the control against which Method 2 was compared. Table 6 includes the data from both techniques for comparison.

Table 6: Comparing Luminous Flux from Field Measurements (Method 1) and HDR Image Coordinates (Method 2)

Target Point	notes	Method 2 Paper Solid Angle	Method 2 Apparent Area (m^2)	Method 1 Apparent Area (m^2)	Mean Luminance (cd/m^2)	Method 2 Luminous Flux to to paper (lumens)	Method 1 Luminous Flux to paper (lumens)
paper 3	center of paper	0.0021	0.0262	0.0359	212.15	0.0117	0.0198
paper 4	center of paper	0.001	0.0379	0.0566	59.89	0.0023	0.0047
paper 1	center of paper	0.0254	0.0363	0.0304	301.11	0.2777	0.2545
Paper 2	center of paper	0.0034	0.0138	0.0175	301.44	0.0141	0.0280
					Total:	**0.3058**	**0.3070**

Comparing solid angles between techniques showed little variation. Apparent areas had a little more variation between methods but were small enough that any differences did not carry over significantly into the final calculation of luminous flux. Given that each piece of paper was a relatively small portion of the image as a whole, some error was expected in finding these values. Summing the luminous flux found for both methods was a way of balancing out any changes between methods. The total lumen output from all four papers was very similar. Individual lumens may have differed slightly, but the differences were hardly noticeable when added together.

Since both methods returned similar luminous flux values, Method 2 was adopted for the other tests carried out for this paper. Method 2 used pixel locations and areas for finding solid angle, and then used the solid angle and photogrammetry to find the apparent area. As long as the location of the camera is known, the reference point coordinates for photogrammetry calculations can be estimated without any additional field measurements, as was the case for the office lighting analysis discussed in section 3.4. However, since there is no meter available to measure the lumen output in a room, another experiment was devised to see if the luminous flux calculated this way was accurate.

3.3 VERIFICATION

Currently, the only tool available to measure lumens is an integrating sphere. These tools are used to measure the total lumen output of lamps or luminaires. They cannot be used to measure a room the way the pilot study did. This is because the HDR method only measures the lumens output in a certain direction, which is the direction of the camera. It is possible, though, to test the HDR imaging method by using an integrating sphere.

This test was conducted to compare the amount of lumens the camera would capture, and compare that with what would be expected for the portion of the integrating sphere that is visible to the camera. The total interior surface of the sphere reflects the total amount of light output from the lamp, in this case a small LED. The camera would only capture a part of the entire sphere, so only a part of the total lumens can be calculated.

A 50*cm* integrating sphere was used to measure the total lumens of a small LED light. The sphere returned a value of 503.2 lumens. The HDR image was expected to only measure a small portion of that. The camera was placed with the lens at a 3" diameter opening in the sphere, and the series of LDR images were taken and then compiled into an HDR image. Figure 7 shows the set-up of this test, and Figure 8 shows the final HDR image of the inside of the integrating sphere.

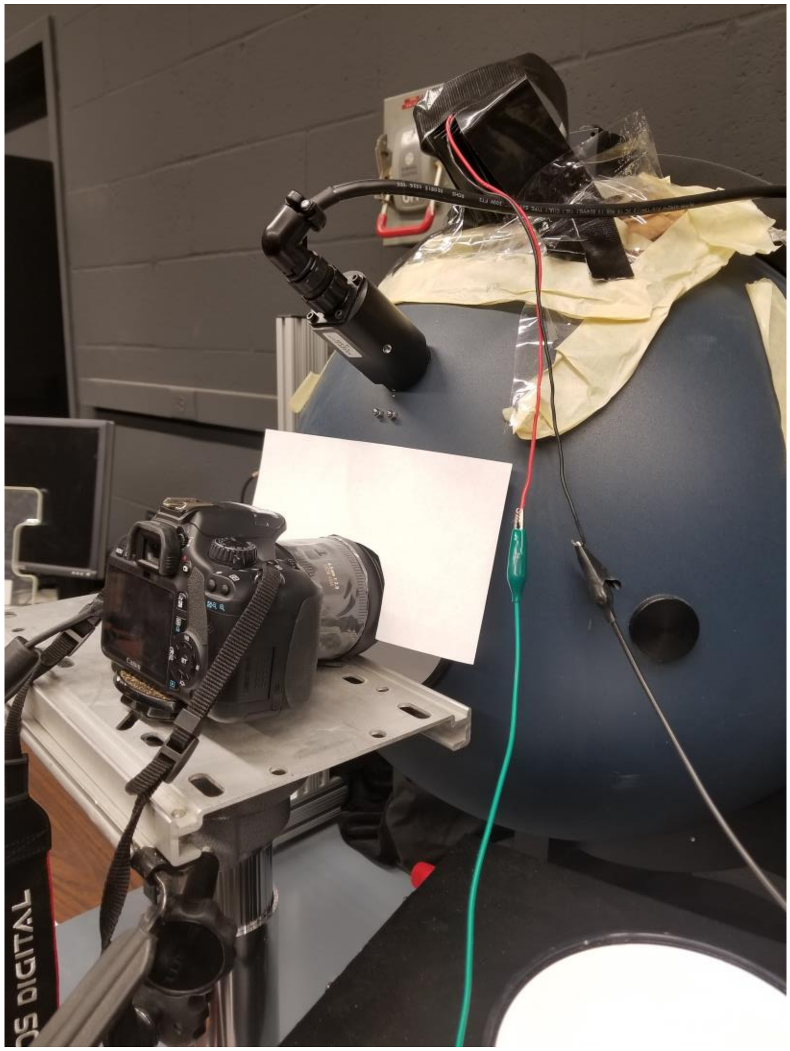

Figure 7: Set-up of validation test

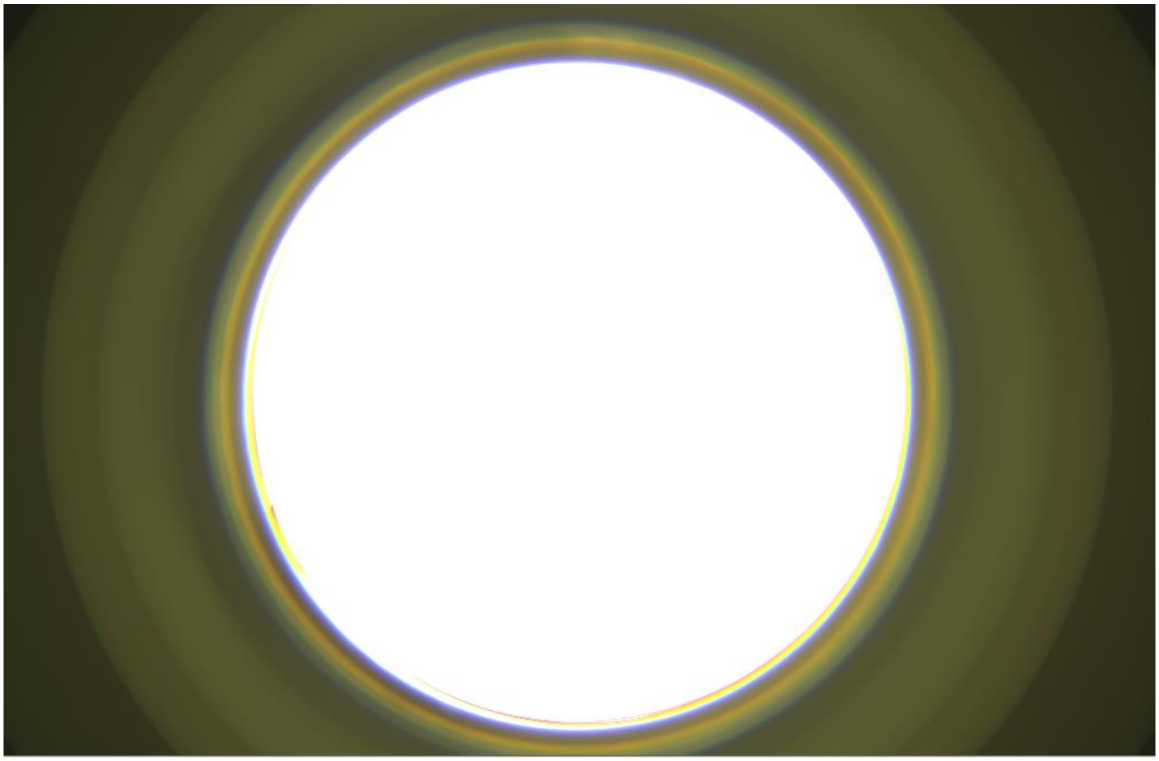

Figure 8: HDR image of inside of integrating sphere

The next step was to find out how many lumens would be expected from the image. Referring back to Figure 3, and the nature of solid angles, the solid angle found in the calculation of lumens is part of a large sphere with the camera at the center. It is worth conceptualizing the camera at the center of a very large integrating sphere, with the luminance calculated from the HDR image in Figure 8. The fraction of the total lumens that would be expected would be the ratio of the surface area of the spherical cap that the camera sees, to the total area of the theoretical sphere with the camera in the center. This is the same as considering a smaller theoretical sphere, with a radius of the camera lens length. Figure 9 shows a two-dimensional representation of this theory. The luminance should remain the same for these theoretical spheres as in the integrating sphere.

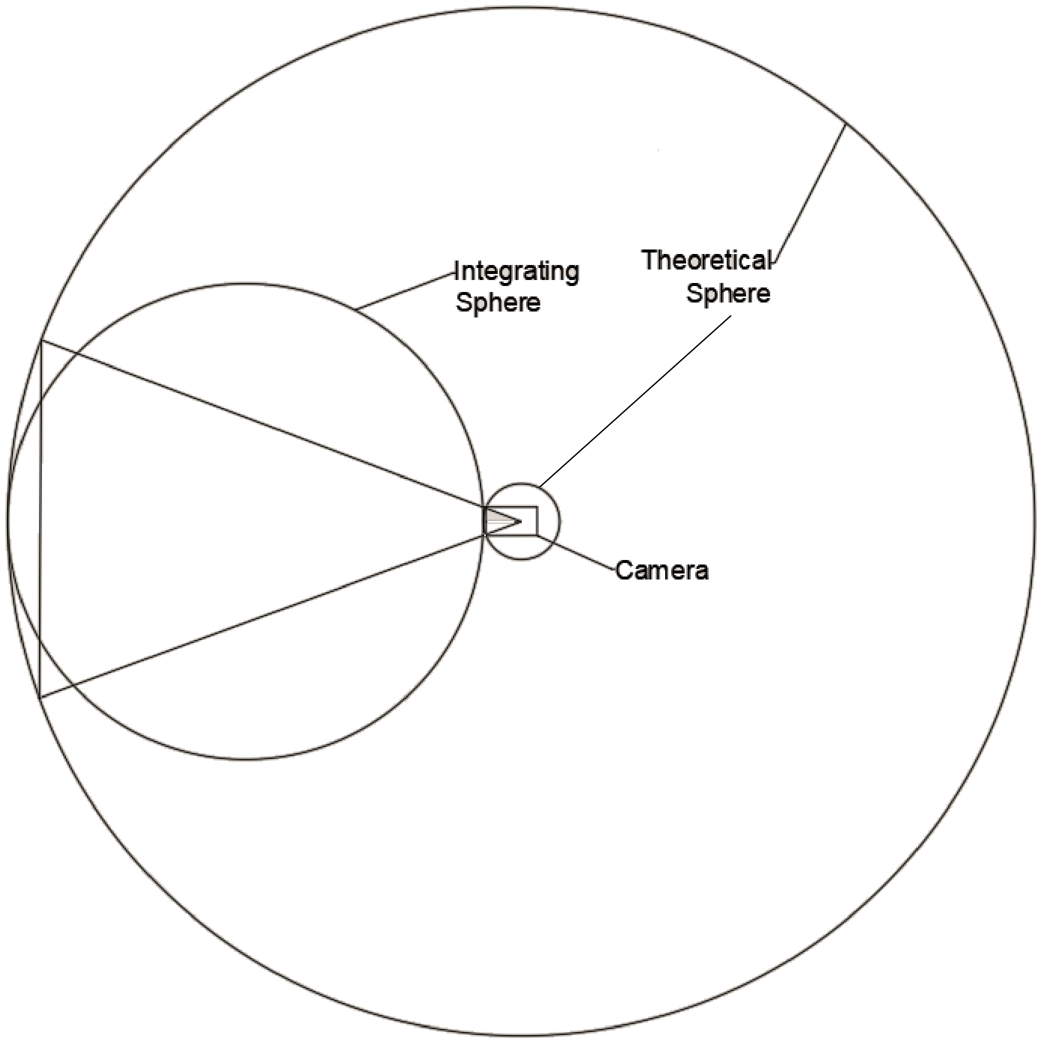

Figure 9: 2-Dimensional conceptualization of validation test

The ratio of the spherical cap to the total theoretical sphere area was 0.030359. In other words, the HDR image was expected to only see about 3.04% of the total 503.2 lumens, which amounts to 15.28 lumens.

Next was to use the HDR image to calculate the lumens using luminance, solid angle, and apparent area. HDRscope provided a mean luminance of 8233 cd/m^2. The camera lens only saw the 3" hole through which it was looking, so the apparent area was the area of that circular hole, or 0.00456 m^2. Combined with the corresponding solid angle of 0.3815, the number of lumens calculated were 14.32 lumens.

The difference between the expected and calculated lumens was only 6.2%, which proved that the lumens calculated using luminance, apparent area, and solid angle were accurate with the true lumen output.

3.4 OFFICE LIGHTING ANALYSIS

3.4.1 SET-UP AND INTRODUCTION

With the method established and verified, the main test of this paper was to apply the procedure to a set of HDR photographs. These photographs were taken as part of a previous experiment by Li (2013) on office ergonomics under different lighting conditions. The experiment was conducted in a small personal office space under four different lighting conditions. Fluorescent lighting was used in the main ceiling luminaires, as well as in the task lighting at the desk in the office for half of the experiment, followed by replacing all the light fixtures with comparable LED fixtures. For both fluorescent and LED lighting, dimming was available, but not always allowed to be used. Two scenarios were tested under each type of light, one scenario without access to dimming for the test subject, and one where the test subject was allowed to dim the lights. This amounted to four different lighting scenarios. Thirty subjects were tested in each of these four settings, and an HDR photograph was taken at the start of each test session, leading to a total of 120 HDR images.

Each HDR image was taken from the point of view of the test subject. The subject's task was to rest their chin on a custom-built chin rest and perform various typing and color matching tests. The results of this experiment are found in Li's past Master's thesis work (2013). Figure 10 shows one of the HDR images of the office set-up that was analyzed.

Figure 10: Typical HDR image of office used in this study

Each image was treated as the same in regards to apparent areas and solid angles. In reality, it was impossible to ensure the same image over 120 separate and distinct instances. The desk and computer screen never moved, but the floor lamp, keyboard, mouse and color checker board differed slightly from image to image. It was assumed that any movement in these elements of the scene would not greatly affect the apparent areas, solid angles, or ultimately the luminous flux. The chin rest also moved from individual to individual, thus meaning a slightly different height of the camera. It was also assumed that any differences in the chin rest and camera location were small enough to not carry over into the results in any drastic way.

3.4.2 IMAGE ANALYSIS

The process used to analyze each of the HDR images of the office matched that of Method 2 of the pilot study. One image was used as the basis for determining apparent areas and solid angles. Only luminance changed from image to image.

Figure 10 is the image of the office for Subject 1 under fluorescent lighting, without subject access to dimming, and was used as the basis for determining area and solid angles. Since apparent areas are dependent on solid angles, the solid angles were found first.

Using the same concept as in the pilot study, the area that different surfaces and objects occupy on the camera's imaging sensor needed to be found. AutoCAD was a valuable tool for finding these areas, since many of them were in odd shapes. The outlines of the different areas of interest were redrawn into AutoCAD in the scale of the imaging sensor. Since the sensor was known to be 14.9 mm x 22.3 mm, and the pixel coordinates could be found in HDRscope, the outline was recreated in AutoCAD, which could then easily provide the area, in mm^2, that was used to find solid angle.

Using the polygonal selection tool in HDRscope, a general outline was made of each major surface and object. Figure 11 shows a sample of the polygon selection tool available in HDRscope. As the polygon was sketched in HDRscope, each pixel coordinate of a joint in the outline was converted into an x, y coordinate in *mm* on the imaging sensor and so drawn into AutoCAD. The final AutoCAD representation of the HDR image is shown in Figure 12.

Figure 11: Sample HDRscope polygon selection area (dotted line)

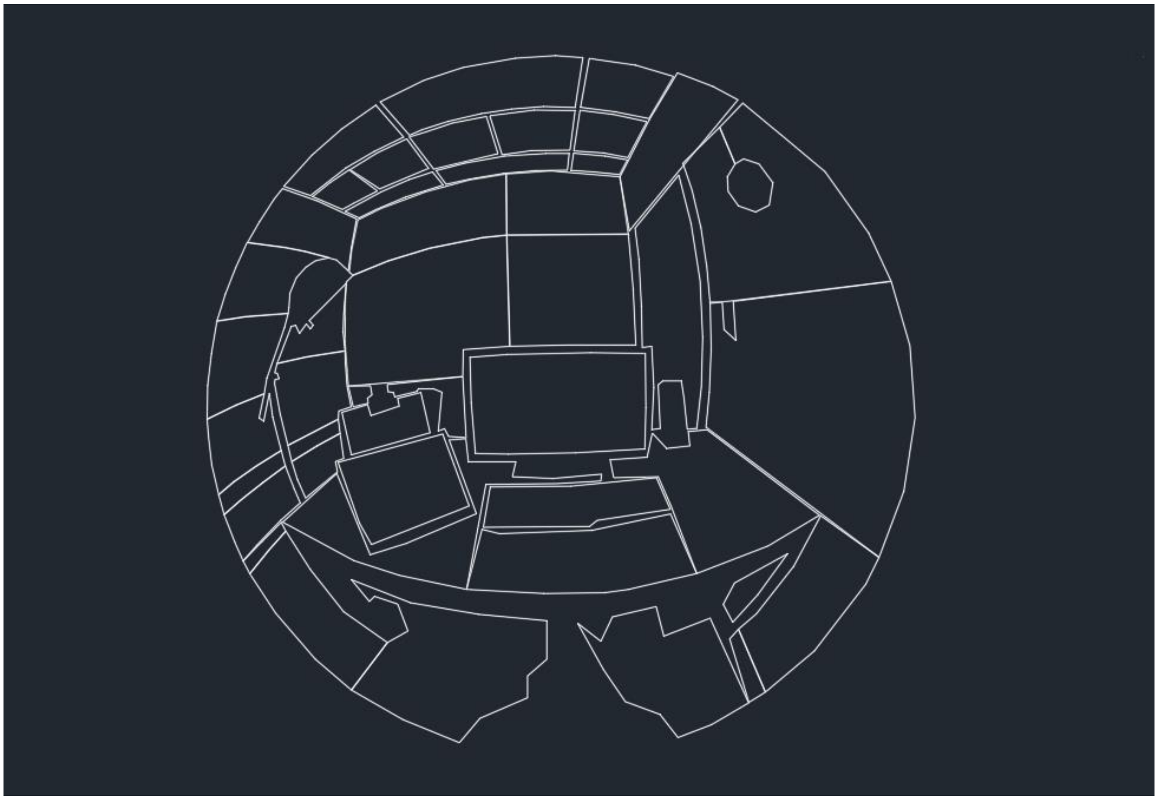

Figure 12: AutoCAD recreation of relevant areas on imaging sensor

Some areas, such as the walls, were divided into smaller areas for increased accuracy. For each of these, the geometric center point could be found as well. The relationship between the center pixel of the individual area and the center pixel of the entire imaging sensor could be used to find the distance, r_2, from the focal point to the center of the area. This distance, in *mm*, was used with the area, in mm^2, in Equation 7 to find the solid angle. This was the same procedure that was proven effective in the pilot study.

With the solid angle of each outlined area known, the next step was to find the apparent area using Equation 6. The distance, r_1, for this equation was the physical distance from the camera lens to the center of the area. Photogrammetry provided this value based on the image pixel coordinates of the area. However, the photogrammetry calculations needed the distances to reference points on each plane. Each wall, the ceiling, the floor, and the desk are different planes in the image. Corners of the walls, ceiling tiles, and other easily measured points were taken as the reference points for these planes. Since the HDR images were taken several years before this analysis, the exact set-up could not be recreated in-person to do the measurements for the reference points. Instead, Revit was used to draw out the office as it was used, based on the floor plan provided by the previous study (Li, 2013). Figure 13 shows the plan layout of the office when the images were taken (the 8 sample points were not relevant for this study). This was re-drafted in Revit, as in Figure 14, so more dimensions could be determined for the relevant reference points for the photogrammetry calculations.

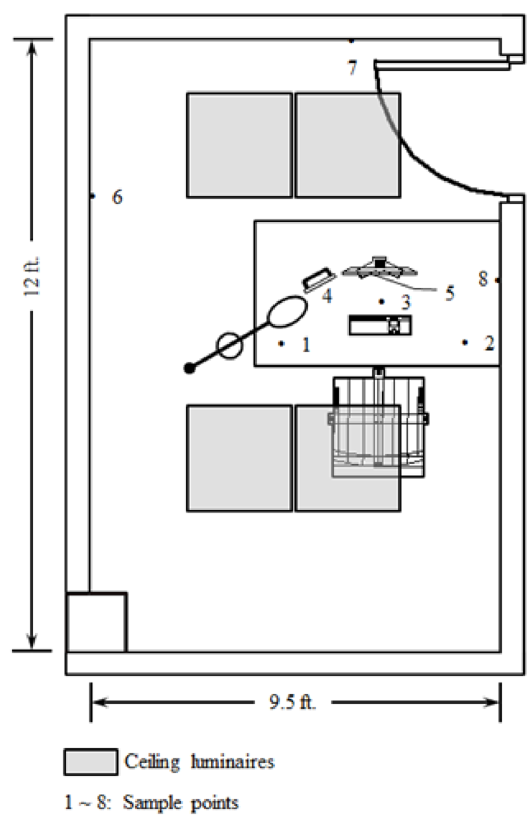

Figure 13: Plan of the office space (Li, 2013)

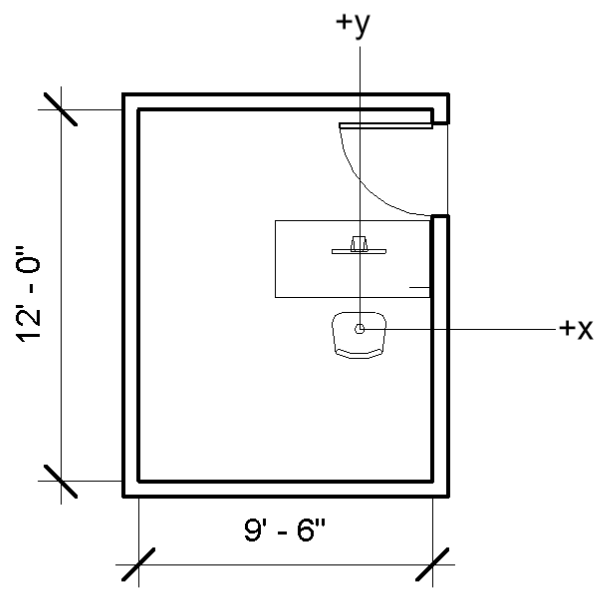

Figure 14: Revit recreation of office for photogrammetry calculations

The center point of the coordinate system had to be estimated to approximately where the camera was. Figure 14 shows the location of the center of the photogrammetry coordinate system. The height, Z, of the camera was estimated as well, using the known height of the table and the average height of the chin rest. Each test subject had a slightly different chin rest measurement, as record by Li (2013) for his initial experiment.

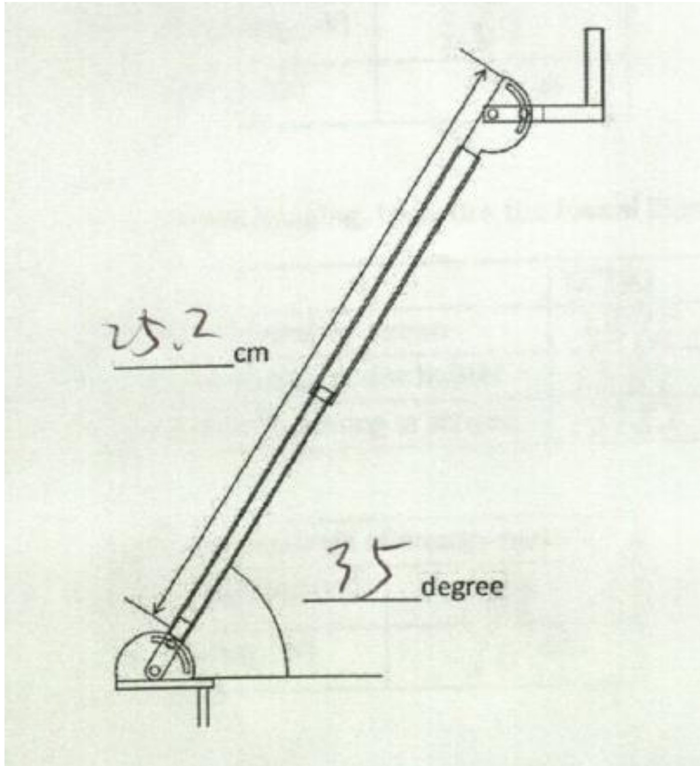

Figure 15: Sample of chin rest measurements to set height, Z, in photogrammetry calculations (Li, 2013)

The average of each of these chin rest heights was taken as 189.9 mm. Combined with the height of the table, and an estimated height from the chin to eye level of 5" (133.3 mm), the camera was estimated at a height of 3.58 ft (1091.6 mm). With the center of the coordinate system set, the X, Y, and Z distances to the reference points were measured in Revit and used to establish the planes in the photogrammetry calculations. Finally, the image pixel coordinates of each area were applied to the photogrammetry template and returned estimates of the physical distance from the camera to the area. This distance was substituted as r_1 in Equation 6 and used with the previously determined solid angle to return the apparent area.

As mentioned previously, some of these areas changed slightly from subject to subject. However, this process was too involved to repeat 119 more times in the time frame of this study. Therefore, it was much easier to assume that the apparent areas and solid angles did not change from subject to subject, and only luminance might change as lighting conditions changed. To fully analyze all 120 images, the mean luminance of each area was measured in HDRscope and then multiplied with the corresponding constant apparent area and solid angle.

The final step in analyzing the HDR photographs is to associate each calculated lumen value with the electrical power usage. A wattmeter was attached to the ceiling luminaires and the floor lamp in the previous study (Li 2013). The energy readings were recorded for each lighting scenario for each test subject. Figure 16 shows some samples of the recorded energy readings. One reading is for the lighting without control, and the other readings are when the test subject dimmed the light to their liking.

record the readings of energy meters	
general lighting (W)	64
task lighting (W)	7.6

(a) Without access to continuous dimming control

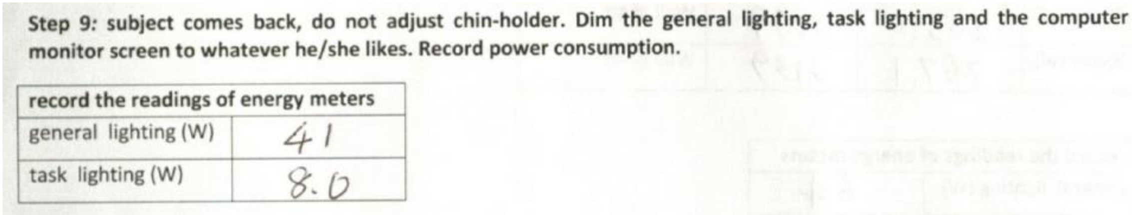
Step 9: subject comes back, do not adjust chin-holder. Dim the general lighting, task lighting and the computer monitor screen to whatever he/she likes. Record power consumption.

record the readings of energy meters	
general lighting (W)	41
task lighting (W)	8.0

(b) With access to continuous dimming control

Figure 16: Wattmeter readings for office lighting for different lighting scenarios for one subject (Li, 2013)

The lumens and associated energy readings were then plotted for all four scenarios: LED with and without access to dimming controls, and fluorescent with and without access to dimming controls. The trends of lumens and wattage were compared, as well as any differences between light sources. These results are discussed more in depth in the next chapter.

CHAPTER 4 DATA ANALYSIS AND RESULTS

Following the procedure outlined in section 3.4, the total lumens output from every major item visible to the camera in the office setting were calculated in excel spreadsheets (see appendices for more detail). Some surfaces contributed no discernable lumens and were typically either very small or very dark surfaces. The floor lamp, computer hard drive, and speakers, for example, were small compared to other surfaces, and measured only a few cd/m^2, that they were excluded from the calculations to simplify and speed up the process. Small sections of the gray trim around the bottom of the walls were used as a basis for excluding similar elements. The sections of trim had such small areas and solid angles, and such low luminance, that they consistently returned values of 0.000 lumens.

The 120 images were analyzed in 4 separate Excel spreadsheets. These Excel spreadsheets are attached separately in the Appendices. Each of the 4 spreadsheets contains a tab for each of the 30 test subjects. The HDR images were grouped by when in the course of the previous study they were taken (Li, 2013), and the spreadsheets were arranged according to this order in which the images were taken. Table 7 lists which of the Excel files contains the luminous flux calculations for each subject in each lighting scenario. Fluorescent_1, for example, is the file for the first HDR image taken for the test subject under fluorescent lighting. Fluorescent_2 was the second HDR image taken under fluorescent lighting for the subject. Half of the subjects were allowed to dim the light first, before coming back and repeating the test under a set lighting level. The other half of the subjects were able to dim light for the second image taken under each lighting type. It is important to pay attention to which lighting scenario is in which Excel file in the Appendices to account for these switches.

Table 7: Excel File in Appendices for Luminous Flux Calculation for Each Lighting Scenario

	Excel Spreadsheet for Each Scenario/Subject			
	Fluorescent Lighting		**LED Lighting**	
Subject	**With Access to Control**	**Without Access to Control**	**With Access to Control**	**Without Access to Control**
1	Fluorescent_1	Fluorescent_2	LED_1	LED_2
2	Fluorescent_1	Fluorescent_2	LED_1	LED_2
3	Fluorescent_1	Fluorescent_2	LED_1	LED_2
4	Fluorescent_1	Fluorescent_2	LED_1	LED_2
5	Fluorescent_1	Fluorescent_2	LED_1	LED_2
6	Fluorescent_1	Fluorescent_2	LED_1	LED_2
7	Fluorescent_1	Fluorescent_2	LED_1	LED_2
8	Fluorescent_1	Fluorescent_2	LED_1	LED_2
9	Fluorescent_1	Fluorescent_2	LED_1	LED_2
10	Fluorescent_1	Fluorescent_2	LED_1	LED_2
11	Fluorescent_1	Fluorescent_2	LED_1	LED_2
12	Fluorescent_1	Fluorescent_2	LED_1	LED_2
13	Fluorescent_1	Fluorescent_2	LED_1	LED_2
14	Fluorescent_2	Fluorescent_1	LED_2	LED_1
15	Fluorescent_2	Fluorescent_1	LED_2	LED_1
16	Fluorescent_2	Fluorescent_1	LED_2	LED_1
17	Fluorescent_2	Fluorescent_1	LED_2	LED_1
18	Fluorescent_2	Fluorescent_1	LED_2	LED_1
19	Fluorescent_2	Fluorescent_1	LED_2	LED_1
20	Fluorescent_2	Fluorescent_1	LED_2	LED_1
21	Fluorescent_2	Fluorescent_1	LED_2	LED_1
22	Fluorescent_2	Fluorescent_1	LED_2	LED_1
23	Fluorescent_2	Fluorescent_1	LED_2	LED_1
24	Fluorescent_2	Fluorescent_1	LED_2	LED_1
25	Fluorescent_2	Fluorescent_1	LED_2	LED_1
26	Fluorescent_2	Fluorescent_1	LED_2	LED_1
27	Fluorescent_2	Fluorescent_1	LED_2	LED_1
28	Fluorescent_1	Fluorescent_2	LED_1	LED_2
29	Fluorescent_2	Fluorescent_1	LED_2	LED_1
30	Fluorescent_1	Fluorescent_2	LED_1	LED_2

Table 8 shows a sample of the calculations for test subject 1, under fluorescent lighting, without any access to dimming control (from Fluorescent_1). The sections of gray wall trim that contributed almost nothing to total lumens were on the right and left walls. The largest contributor of light across all images was the whiteboard, regardless of not having the highest luminance. The ceiling luminaires understandably had the highest luminance, but relatively smaller apparent areas and solid angles, thus attributing fewer lumens to the camera.

Table 9 shows the results for the same test subject, but under LED lighting, without access to dimming control (from LED_1). There were some noticeable differences in the individual areas between fluorescent and LED. Namely, the ceiling luminaires under LED lighting were consistently much brighter than the fluorescent counterparts. The lumen contribution from them was understandably higher, but the total image lumens remained similar, and even slightly less than the totals under fluorescents.

Table 8: Sample Image Lumen Calculations (Fluorescent, Subject 1, without access to continuous dimming control)

	location	r (for solid angle) (mm)	Distance to lens (m)	distance to lens (ft)	Area on Imaging Sensor (mm^2)	Area's solid angle	Area's Apparent Area (m^2)	Area Luminance (cd/m^2)	Luminous Flux Due to Area (lumen)
Computer	Computer Screen	4.501	0.737	2.417	4.7933	0.237	0.128	311.05	9.450
Front wall w/ whiteboard	Whiteboard	5.280	2.607	8.554	5.4719	0.196	1.334	136.66	35.786
	Front wall, under board, left	5.623	2.927	9.604	0.1025	0.003	0.028	53.21	0.005
	Front wall, under board, right	4.922	2.372	7.781	0.5378	0.022	0.125	60.87	0.169
	Front bare wall (above computer)	4.918	2.364	7.755	3.8607	0.160	0.892	77.91	11.087
	Front bare wall (right corner)	5.465	2.758	9.050	2.017	0.068	0.514	85.90	2.981
	Front bare wall (top of board)	5.476	2.769	9.083	2.4784	0.083	0.634	245.39	12.852
Right Wall	above door	6.616	2.068	6.785	2.1436	0.049	0.209	69.05	0.708
	door	5.199	1.871	6.137	3.1501	0.117	0.408	56.99	2.708
	right of door, no clock, above switch	6.523	1.101	3.611	6.4721	0.152	0.184	104.59	2.930
	right of door, around swith, above table	6.254	0.861	2.824	11.3152	0.289	0.214	87.16	5.405
	right of table leg	6.918	0.968	3.175	3.0646	0.064	0.060	48.83	0.188
	under table	6.277	1.197	3.927	0.3699	0.009	0.013	14.29	0.002
	gray trim, right of table	6.998	1.300	4.264	0.2883	0.006	0.010	3.10	0.000
Left Wall	upper, above lamp	6.897	2.829	9.282	1.3636	0.029	0.229	112.60	0.741
	left of lamp head	7.035	2.457	8.061	1.3373	0.027	0.163	142.52	0.628
	right of lamp head	6.190	2.785	9.138	0.7155	0.019	0.145	114.06	0.309
	left of diagonal arm	7.026	2.283	7.489	1.5625	0.032	0.165	103.41	0.540
	left, above board	7.013	2.269	7.443	1.2513	0.025	0.131	77.12	0.257
	right, above board	6.145	2.692	8.832	1.4146	0.037	0.271	87.51	0.890
	left board	6.981	2.328	7.638	0.3793	0.008	0.042	71.58	0.024
	right board	6.137	2.713	8.900	0.2251	0.006	0.044	80.03	0.021
	Gray Trim	7.108	2.463	8.080	0.1721	0.003	0.021	3.59	0.000
	left below board	6.956	2.404	7.887	0.9382	0.019	0.112	51.84	0.113
	right below board	6.136	2.762	9.063	0.4925	0.013	0.100	55.66	0.073
ceiling	Top right tile	7.085	1.866	6.122	1.0679	0.021	0.074	42.67	0.067
	Top middle tile	7.078	1.881	6.172	2.5689	0.051	0.181	49.80	0.463
	Top Left Tile	7.209	2.356	7.731	1.0936	0.021	0.117	66.96	0.165
	center right tile	6.488	2.054	6.738	0.6817	0.016	0.068	47.24	0.052
	center middle tile	6.491	2.033	6.671	0.8639	0.021	0.085	60.63	0.105
	center left tile	6.825	2.676	8.781	0.359	0.008	0.055	76.47	0.033
	right front tile	6.118	2.244	7.362	0.2415	0.006	0.032	41.46	0.009
	middle front tile	6.132	2.270	7.447	0.6011	0.016	0.082	70.67	0.093
	Left front tile	6.384	2.615	8.580	0.3742	0.009	0.063	88.28	0.051
	Left Luminaire	6.810	2.292	7.521	0.5611	0.012	0.064	2951.35	2.270
	Right Luminaire	6.568	2.140	7.021	0.8029	0.019	0.085	2981.46	4.731
floor	right of chin rest	6.204	1.458	4.784	3.4663	0.090	0.192	11.76	0.203
	left of chin rest to table edge	6.505	1.334	4.376	4.9179	0.116	0.207	24.29	0.584
	left of table	7.008	1.756	5.762	2.3546	0.048	0.148	36.60	0.259
Table	under computer, right of keyboard	5.430	1.081	3.546	3.8716	0.131	0.153	23.83	0.480
	under keyboard, no chin rest	5.179	0.640	2.100	3.6849	0.137	0.056	30.42	0.235
	under computer, left of keyboard	14.102	0.870	2.854	2.9468	0.015	0.011	44.45	0.007
	keyboard	4.782	0.982	3.223	1.9016	0.083	0.080	9.10	0.061
color checker	color checker	5.385	0.752	2.467	2.5037	0.086	0.049	32.67	0.138
Paper on stand	paper on stand	14.145	0.840	2.755	0.8981	0.004	0.003	214.81	0.003
								Total	**97.875**

Table 9: Sample Image Lumen Calculations (LED, Subject 1, without access to continuous dimming control)

	location	notes	r (for solid angle) (mm)	Distance to lens (m)	distance to lens (ft)	Area on Imaging Sensor (mm^2)	Area's solid angle	Area's Apparent Area (m^2)	Area Luminance (cd/m^2)	Luminous Flux Due to Area (lumen)
Computer	Computer Screen		4.501	0.737	2.417	4.7933	0.237	0.128	254.90	7.744
Front wall w/ whiteboard	Whiteboard		5.280	2.607	8.554	5.4719	0.196	1.334	134.75	35.286
	Front wall, under board, left		5.623	2.927	9.604	0.1025	0.003	0.028	56.62	0.005
	Front wall, under board, right		4.922	2.372	7.781	0.5378	0.022	0.125	67.84	0.188
	Front bare wall (above computer)		4.918	2.364	7.755	3.8607	0.160	0.892	71.82	10.221
	Front bare wall (right corner)		5.465	2.758	9.050	2.017	0.068	0.514	62.42	2.166
	Front bare wall (top of board)		5.476	2.769	9.083	2.4784	0.083	0.634	193.79	10.150
Right Wall	above door		6.616	2.068	6.785	2.1436	0.049	0.209	59.61	0.612
	door		5.199	1.871	6.137	3.1501	0.117	0.408	52.71	2.505
	right of door, no clock, above switch		6.523	1.101	3.611	6.4721	0.152	0.184	94.97	2.661
	right of door, around swith, above table		6.254	0.861	2.824	11.3152	0.289	0.214	81.81	5.073
	right of table leg		6.918	0.968	3.175	3.0646	0.064	0.060	48.72	0.187
	under table		6.277	1.197	3.927	0.3699	0.009	0.013	8.65	0.001
	gray trim, right of table		6.998	1.300	4.264	0.2883	0.006	0.010	3.50	0.000
Left Wall	upper, above lamp		6.897	2.829	9.282	1.3636	0.029	0.229	123.02	0.809
	left of lamp head		7.035	2.457	8.061	1.3373	0.027	0.163	118.22	0.521
	right of lamp head		6.190	2.785	9.138	0.7155	0.019	0.145	102.30	0.277
	left of diagonal arm		7.026	2.283	7.489	1.5625	0.032	0.165	90.04	0.470
	left, above board		7.013	2.269	7.443	1.2513	0.025	0.131	73.14	0.244
	right, above board		6.145	2.692	8.832	1.4146	0.037	0.271	80.91	0.823
	left board		6.981	2.328	7.638	0.3793	0.008	0.042	70.85	0.023
	right board		6.137	2.713	8.900	0.2251	0.006	0.044	79.80	0.021
	Gray Trim		7.108	2.463	8.080	0.1721	0.003	0.021	3.00	0.000
	left below board		6.956	2.404	7.887	0.9382	0.019	0.112	50.26	0.109
	right below board		6.136	2.762	9.063	0.4925	0.013	0.100	56.26	0.073
ceiling	Top right tile		7.085	1.866	6.122	1.0679	0.021	0.074	38.61	0.061
	Top middle tile		7.078	1.881	6.172	2.5689	0.051	0.181	45.34	0.422
	Top Left Tile		7.209	2.356	7.731	1.0936	0.021	0.117	63.71	0.157
	center right tile		6.488	2.054	6.738	0.6817	0.016	0.068	42.35	0.047
	center middle tile		6.491	2.033	6.671	0.8639	0.021	0.085	54.24	0.094
	center left tile		6.825	2.676	8.781	0.359	0.008	0.055	72.13	0.031
	right front tile		6.118	2.244	7.362	0.2415	0.006	0.032	36.50	0.008
	middle front tile		6.132	2.270	7.447	0.6011	0.016	0.082	59.45	0.078
	Left front tile		6.384	2.615	8.580	0.3742	0.009	0.063	72.75	0.042
	Left Luminaire		6.810	2.292	7.521	0.5611	0.012	0.064	5975.37	4.595
	Right Luminaire		6.568	2.140	7.021	0.8029	0.019	0.085	5096.98	8.088
floor	right of chin rest		6.204	1.458	4.784	3.4663	0.090	0.192	12.69	0.219
	left of chin rest to table edge		6.505	1.334	4.376	4.9179	0.116	0.207	26.84	0.645
	left of table		7.008	1.756	5.762	2.3546	0.048	0.148	31.35	0.222
Table	under computer, right of keyboard		5.430	1.081	3.546	3.8716	0.131	0.153	20.96	0.422
	under keyboard, no chin rest		5.179	0.640	2.100	3.6849	0.137	0.056	22.61	0.175
	under computer, left of keyboard		14.102	0.870	2.854	2.9468	0.015	0.011	45.45	0.008
	keyboard		4.782	0.982	3.223	1.9016	0.083	0.080	12.38	0.083
color checker	color checker		5.385	0.752	2.467	2.5037	0.086	0.049	34.89	0.147
Paper on stand	paper on stand		14.145	0.840	2.755	0.8981	0.004	0.003	249.77	0.004
									Total	**95.715**

Special care needed to be taken to understand which lighting scenario was being calculated, and which energy reading corresponded to which image. Four HDR images were taken per test subject, one for each lighting scenario, which had to be correctly paired with the corresponding energy usage. Table 10 includes the calculated lumens for all subjects and scenarios, and the associated wattage. The wattage shown in Table 10 includes wattage for both the ceiling luminaires and the floor lamp.

Table 10: Lumens and Wattage Results

Subject	Without Control					With Control			
	Fluorescent (lumens)	Energy Usage (W)	LED (lumens)	Energy Usage (W)		Fluorescent (lumens)	Energy Usage (W)	LED (lumens)	Energy Usage (W)
1	97.875	171.9	95.715	71.6		72.484	146.5	65.614	49
2	107.477	175.5	93.452	71.4		45.75	159.7	88.958	69
3	101.343	169.8	96.344	70.3		45.036	154.8	80.565	41.5
4	112.749	182	94.561	65		108.57	180.7	82.368	59.5
5	104.991	170.8	90.507	67.7		123.681	189.3	117.137	89.2
6	109.395	185	81.878	66.7		16.685	169.4	17.311	25.2
7	94.63	172.6	95.137	67.4		5.856	104.6	82.711	68.1
8	100.334	176	90.789	67.2		13.785	135	31.172	45.2
9	102.776	170.4	93.847	67.8		11.777	128	12.154	19.8
10	106.768	181.1	95.28	67.2		13.698	131.3	113.568	40.6
11	99.81	171.1	92.885	67.2		132.253	204.5	106.708	79.2
12	99.392	168.5	94.313	69.3		41.663	152	52.461	36
13	106.216	176.4	89.586	68		133.757	177.5	130.935	96
14	109.881	174.8	100.746	67.7		100.299	171.7	75.264	57.6
15	111.499	182	97.619	67.5		126.367	199	75.864	55.3
16	106.268	174.3	99.014	67.2		98.543	184.9	78.944	58.4
17	100.889	170.7	101.104	71.5		133.728	219	129.499	89.7
18	104.19	171.3	95.359	67.5		133.429	213	76.596	59.9
19	94.581	165.7	97.552	68		78.801	153.6	82.676	68.4
20	102.874	174.7	93.231	67.2		39.97	158.6	126.511	92.8
21	102.029	169	94.083	65.5		13.374	129.3	6.554	17.5
22	100.946	176.2	94.313	66.8		5.455	127.9	39.263	42.7
23	102.972	175.2	90.956	66.7		40.017	156.8	25.348	38.7
24	104.54	170.7	101.11	68.2		47.738	157.5	65.201	47.3
25	101.047	167.8	96.8	67.2		87.758	160.8	52.027	39
26	105.16	173.7	98.166	67.2		45.691	160.8	29.724	21
27	105.379	176	90.832	66.5		46.069	157.1	89.053	62.5
28	109.491	176.8	101.011	67.5		119.96	183.5	127.368	84.6
29	106.972	175.7	99.19	66		30.454	136.5	64.011	47
30	98.912	174.5	94.071	67.2		26.012	130.1	77.53	54.2
AVG	**103.713**	**174.007**	**94.982**	**67.740**		**64.622**	**161.113**	**73.437**	**55.163**

It was expected that without access to dimming control, the lumens from subject to subject would remain relatively constant, as would wattage. When the test subject was allowed to dim the lighting to their desired level, the lumens would change, but the wattage should follow the change of the lumens. Since lumens are the lighting energy output, conservation of energy implies that the output should be at least proportional to the energy input. LEDs are also more energy efficient than fluorescents, so the electrical energy usage should be much less than fluorescents. The results presented in Table 10 confirm all these hypotheses.

There were some issues with some of the data points which are worth mentioning. Out of all scenarios, there were about two dozen outliers. It is believed that these outliers were caused by an undiagnosed issue with HDRscope. The luminance values per area were different from the rest of the data in the similar setting. The luminance values were checked in Photosphere, another HDR luminance software, which returned luminance values for the outliers similar to their neighbors, as opposed to HDRscope. For example, HDRscope was showing roughly double the luminance for subject 8, under fluorescent lighting without control, than the other subjects in the same lighting conditions. Without lighting control, all luminance values should be the same. Photosphere returned similar luminance values for subject 7, 8, and 9, showing none of the discrepancies apparent in HDRscope. The problem in HDRscope could not be found, and so a small calibration was needed for these couple dozen outliers.

Since Photosphere was returning luminance measurements as expected, it was used as the basis for the calibration. Six points in the office were selected to be measured in both Photosphere and HDRscope. The ratios between the Photosphere luminance and

HDRscope luminance of the same points were calculated for the outlier and the subjects immediately before and after the outlier. The outlier's ratio between Photosphere and HDRscope should be the same as that from the subjects before and after it. A calibration factor was found to correct the luminance measurements from HDRscope so that the outliers matched the other subjects. It seems possible that the magnitude of the lumens may have been different had Photosphere been used for Luminance rather than HDRscope. However, Photosphere is not as friendly to this experiment, as it can only measure rectangular areas, not polygonal areas. Regardless, the verification test proved that the method only had about 6.2% error, and that was with HDRscope. With the outliers fixed, the final lumen values are believed to be as accurate as the verification test. All of the corrected lumen values are shown in Table 10.

Plots of the lumens and wattage give a better visual representation of the correlation between lumens and wattage. Figures 17 and 18 graphically show the wattage and lumens for each lighting scenario. The plots in parts *a* of both figures better show how lumens and power stayed relatively constant without access control. Part *b* of Figures 17 and 18 perhaps show the best correlation between lumens and wattage. Consistently, lumens and wattage decreased as subjects dimmed the lights, and increased as lights were made brighter.

Altogether, this method is a valid procedure for calculating lumens, and can be useful for future research and other applications. Due to some potential problems with HDRscope, it would be best to test this procedure again with a more established and reliable luminance/HDR software, such as Photosphere. Nonetheless, the method and results in this paper present some new facets to HDR imaging as a lighting measurement tool that warrant more investigation and study.

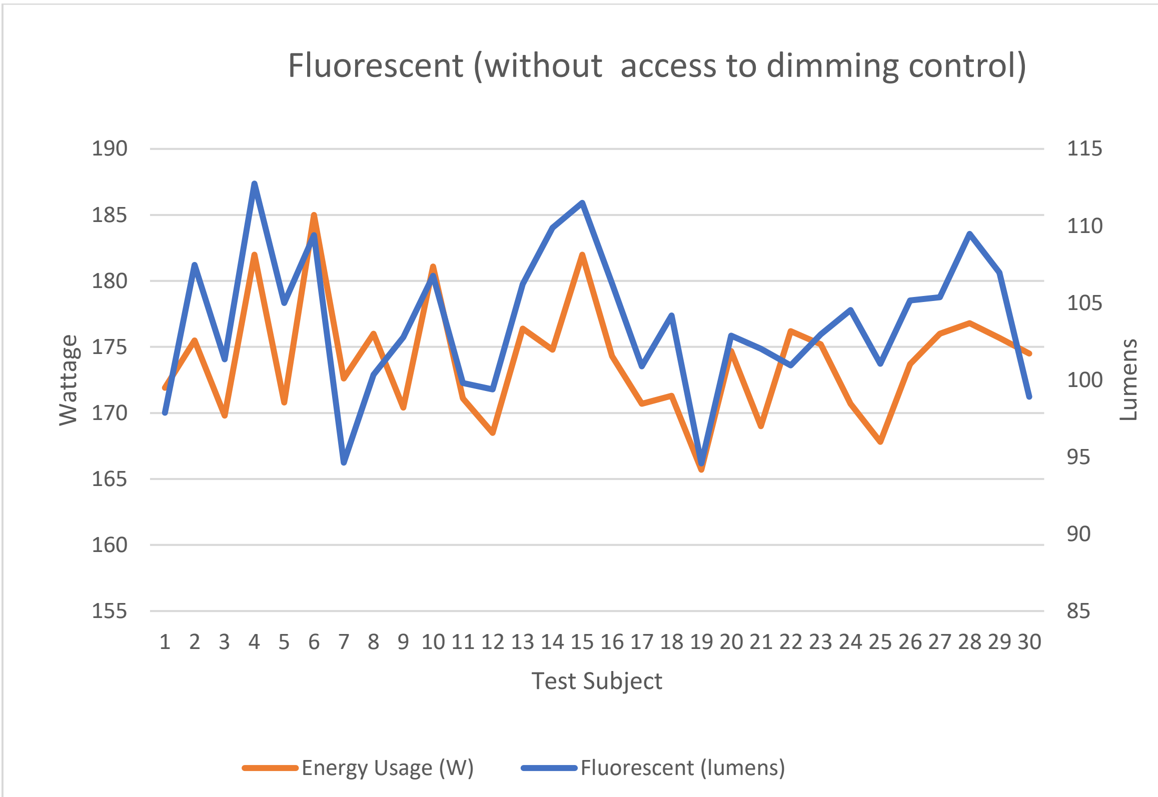

(a)

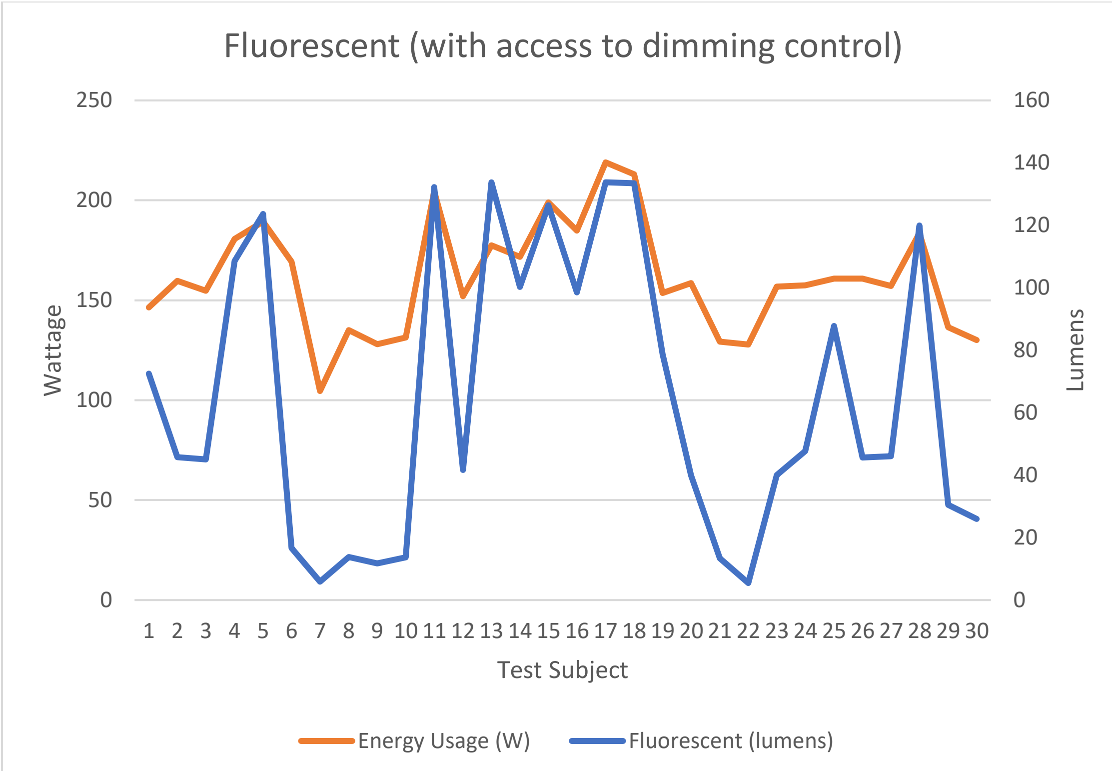

(b)

Figure 17: Fluorescent lumens and wattage (a) Without access to continuous dimming controls, (b) With access to continuous dimming controls

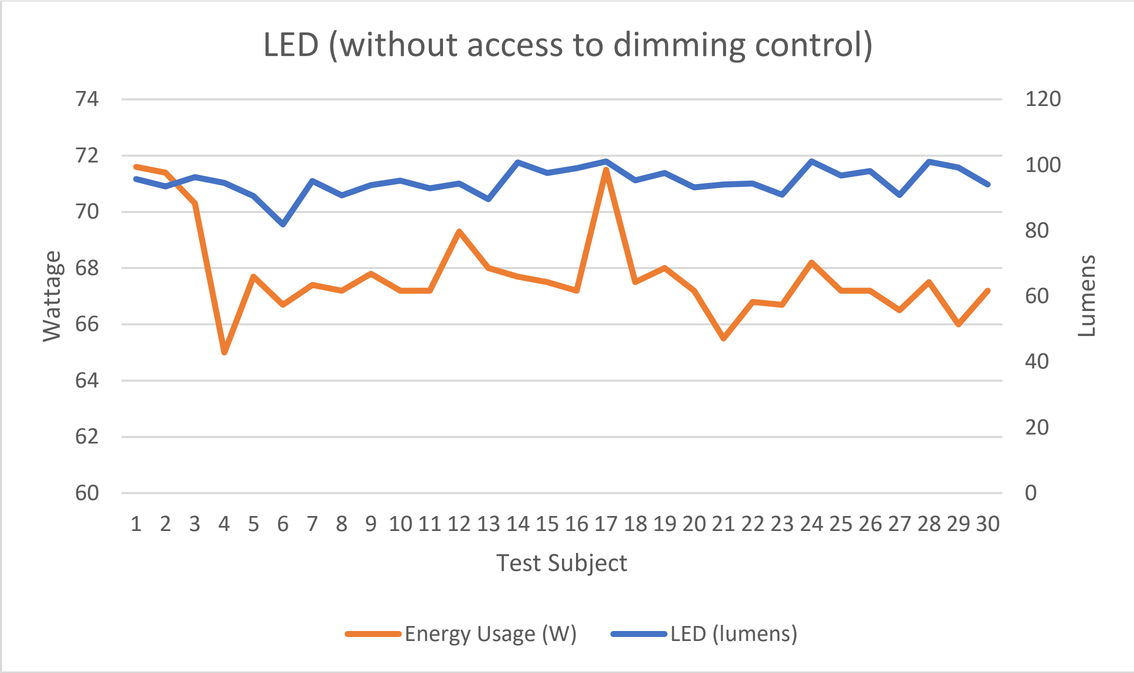

(a)

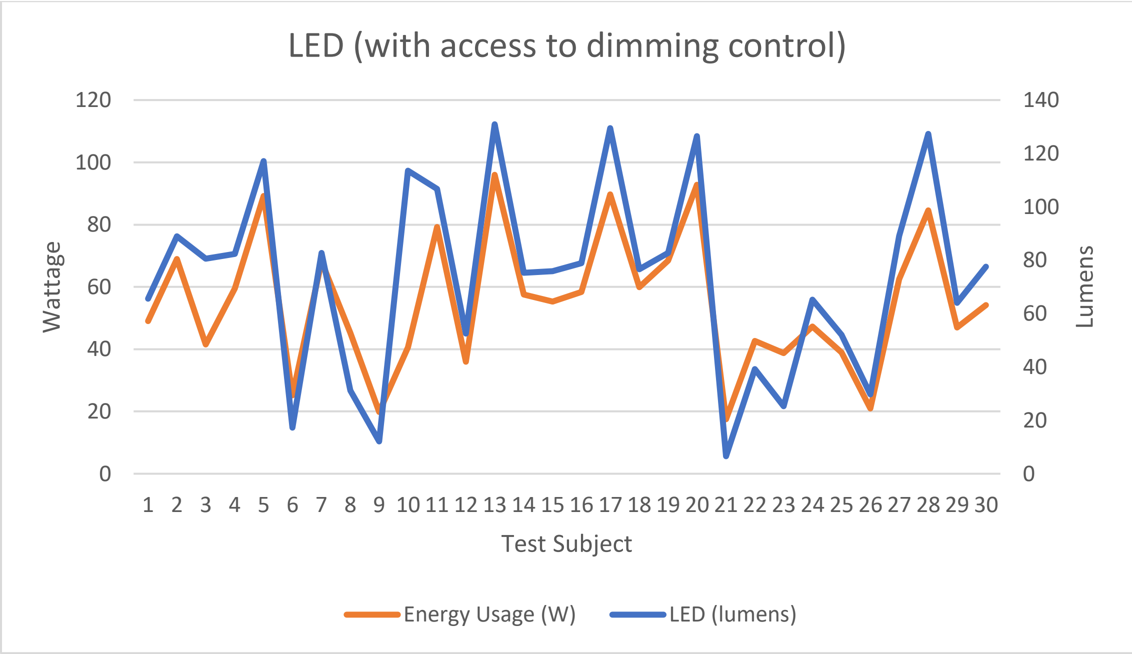

(b)

Figure 18: LED lumens and wattage (a) Without access to continuous dimming controls, (b) With access to continuous dimming controls

CHAPTER 5 CONCLUSIONS AND RECOMMENDATIONS

5.1 Conclusions

High Dynamic Range (HDR) photography is typically used for measurement of luminance and assistance in glare analysis. This study proved that HDR imaging could also be used to estimate directional luminous flux obtained from an HDR image. The camera-aided method developed and tested in this study successfully showed that an HDR image could help determine the amount of lumens reaching the camera lens (or eyes of a space user) contributed from all light sources and surfaces visible to the camera in a space. The validation test proved the method developed in the pilot study is accurate in measuring luminous flux coming to a particular viewpoint with an error of 6.2% when compared to the measurement using an integrating sphere. The office lighting study further validated the method by applying it in an office environment over many HDR images taken under different lighting conditions. Because electrical energy is converted into luminous flux by the lighting system, it was also proven that they would follow the same trend. The results proved that the new process can accurately estimate directional luminous flux that a camera lens (or a space occupant) sees.

This method differs with other's work in that it only finds the lumens output towards the camera lens (or eyes of the space occupant) in a real luminous environment. Other papers have examined using luminance to estimate total luminous flux of a lamp or luminaire in all viewing directions (Fung & Chang 2007; Andreas & Krochman 1986). These papers do not, however, do their measurements in the context of the lamps actively being used in a space. The HDR method finds how many lumens the luminaires output in the direction of the camera, so this can potentially be used to estimate the total number of lumens. Depending on the fraction of the total lumens the camera sees, the total lumens can possibly be found. This can help analyze existing buildings with older luminaires where the data of existing fixtures may not be available.

This study established how to find lumen exposure (or light dosage) to space occupants using HDR photographs, and then used this to examine the wattage and lumen relationship, as well as differences between the lumens of LEDs and fluorescents. This is only the start of how directional luminous flux can be used in research and practice. As a new measurement tool, there is vast potential for using the HDR imaging and the equations developed in this paper for more research and possibly even commercial usage in lighting control.

5.2 Recommendations

There are multiple takeaways from this method concerning how it can be used in the future, including the potential for more practical and commercial uses. With significantly more development, HDR photography can be incorporated into buildings as lighting controls. As HDR images can begin to provide more information than luminance, HDR cameras and images can possibly start to control lighting in a space in consistency with how much light dosage the space occupants are taking over time and space. These cameras can be incorporated with building security cameras and avoid the extra cost of photosensors and the like. A camera can periodically take HDR images of a space and can use computer programs to measure the light in the space with the help of the process developed in this paper. Furthermore, the luminance of surfaces can also be monitored to dim adjacent light sources accordingly.

On the other hand, inserting HDR imaging into lighting controls is not a current goal of the industry and it is possible that it is not ultimately practical. The algorithms would be substantial and require large amounts of room specific data to be pre-programmed. As shown in the photogrammetry alone, reference points need to be known to estimate the distance from the camera to the object in question. Changes in the scenery of the image are also not guaranteed to be as small and insignificant as those present in this study. This means that in practice, the apparent areas and solid angles would constantly change from image to image as people and objects move about the rooms. Measuring lumens would be helpful in lighting control and building automation, though, if these problems are overcome. This paper shows that lumens and power usage are proportionally related, which can be helpful not only in dimming lights, but also monitoring energy used for lighting.

Daylighting is also another factor of light in a space that is not covered by this paper. The office had no windows, and so electrical light only contributed to measured lumens. Electrical lighting is much more consistent in light output than daylight, which is constantly changing, so it might be difficult for HDR cameras to keep up with the ever-changing lighting in a daylit space. All these obstacles imply that using a camera and HDR images in building lighting control is still very far off and may ultimately not be a good solution for lighting control in practice. The answer to that requires much more study and testing of the method presented in this paper, and HDR imaging as a whole. However, it is not altogether improbable to imagine that as technology improves, this lumen calculation method can be incorporated into building control. At the moment, though, HDR photography is more of a helpful research and simulation tool than a potential product to be used in buildings.

Several other potential topics of further research have surfaced just from this paper alone. As mentioned in Chapter 4, some issues arose with a few dozen images when they were measured in HDRscope that did not occur when measured in Photosphere. The particular reason of why these outliers occurred is worth investigating. It also appeared that during the calibration, the two software were returning different luminance values. It remains unclear what caused the difference between these two software packages that are supposed to have the same base code of Radiance. It is also worth wondering how the lumens would be different had Photosphere been used as the luminance tool instead of HDRscope.

There's also potential to make the calculations more accurate. The process of finding the apparent areas and solid angles for one image as discussed in Chapter 3 proved to be exceedingly time consuming and involved. It might be possible to simplify this process with a computer program, so that each image can be processed individually instead of using the same apparent areas and solid angles for each image. As mentioned previously, some items in the office moved. The camera was not always at the same height, and sometimes the areas were in different sizes and shapes than the original. Oftentimes the lumens of those particular areas were so small, that any of these changes in the scene were ultimately not significant in the final total of lumens. As shown in the lighting without access to dimming control, the lumens all stayed relatively close to each other from subject to subject. Any changes such as 94 lumens to 106 lumens are small but are likely due to the differences in the visible surfaces and objects between images. It was not possible in the timeframe of this project to individually calculate apparent areas and solid angles for each image's areas and objects, but it is certainly possible that this process can be automated in some way to speed up the process and provide slightly more accurate results.

Another possibility for this research to be applied is in the study of different materials. Each of the surfaces in an HDR image reflect some of the light that hits them, and so acts as a type of light source. Using these calculations, the amount of light reflected from a surface is measured, giving insight into the properties of different surface finishes. The whiteboard in the office was consistently the largest contributor of lumens, and not the ceiling luminaires as might be assumed. This is mainly due to the larger area that the whiteboard occupies, as opposed to the luminaires. Furthermore, the left wall, made of painted CMU's, had lower lumens than the other walls made of painted drywall. This implies a lower reflectivity between the CMU wall and drywall. It is apparent that these calculations can be used to study different surfaces, and that lumens can be associated with reflectivity. For existing buildings, this can help analyze rooms for suspected changes in light levels due to new paint or finishing.

This paper also merely touches on the relationship between watts and visible lumens. It is clear that the two are proportionally related, but further study can more closely study this relationship. It might be possible that the wattage can be estimated from the calculated lumens, or vice versa, but it remains to be seen how that could be accomplished. This test considers only two types of light sources, fluorescent and LED with similar distribution patterns. Lumens reflected from the room's surfaces would likely change as luminaire distribution patterns change. Not all luminaires emit light in the same intensity in all directions, so light would be reflected differently throughout a room. The effect that this has on the measured lumens should be studied further, as well as how that changes the correlation with wattage, if at all. It is likely that lumens and wattage will still increase and decrease together, but the difference in magnitude of power and lumens might change with light sources.

REFERENCES

Andreas, Brazel, & Krochman, Juergen. 1986. "Luminous Flux Measurement." *Licht* 38, no. 2: 136-138, 141. Engineering Village.

Brigham Young University. "Geometry of Radiation." https://www.et.byu.edu/~vps/ME340/TABLES/12.0.pdf

Cai, Hongyi, Li, Linjie. 2016. "How LED lighting may affect office ergonomics: The impact of providing access to continuous dimming controls on typing and colour-matching tasks performance." *Light and Engineering* 24, no. 2: 25-36.

Cai, Hongyi, Papamichael, Konstantinos, Inanici, Mehlika, *et. al.* 2017. "Application of High Dynamic Range Imaging in Daylighting Practice: An Outline for a Motion to Set Up a New HDRI Sub-Committee." (unpublished draft)

Cai, Hongyi. 2012. "High Dynamic Range photogrammetry for synchronous luminance and geometry measurement." *Lighting Research and Technology*.

Fung, Rong-Fong, & Chang, Liang-Kang. 2007. "Methods of estimating luminous flux of the backlight module by luminance measurement." *Optical Engineering* 46, no. 1. Compendex.

Kumaragurubaran, Viswanathan, Inanici, Mehlika. 2013. "HDRscope: High Dynamic Range Imaging Processing Toolkit for Lighting Simulations and Analysis." *13th Conference of International Building Performance Simulation Association.*

Kumaragurubaran, Viswanathan, Inanici, Mehlika. HDRscope (2012). University of Washington, 2012. http://courses.washington.edu/hdrscope/

Kumaragurubaran, Viswanathan. 2012. “High Dynamic Range Image Processing Toolkit for Lighting Simlations and Analysis.” MS thesis, University of Washington.

Labsphere, Inc. 2017. “Integrating Sphere Theory and Applications.” *Technical Guide*.

Levin, Robert E. 1968. “Luminance – A Tutorial Paper.” *Journal of SMPTE* 77, no. 10: 1005-1011. IEEE Xplore Digital Library.

Li, Linjie. 2013. “Impact of new lighting technologies on office ergonomics.” MS thesis, University of Kansas.

Moeck, Martin, Anaokar, Smita. 2006. “Illuminance Analysis from High Dynamic Range Images.” *Leukos* 2, no. 3: 211-228. ResearchGate.

Ward, Greg. Photosphere. Anyhere Software, Berkley, CA. http://www.anyhere.com/

Wolpert, H.D. 1983. “Unraveling the Mystery of Integrating Spheres.” *Electro-Optics* 15, no. 8: 39-40. Compendex.

APPENDICES

The total of 120 excel spreadsheets for data treatments are enclosed with this thesis in electronic copy, which is available upon request. Due to their extraordinarily large size, they are not printed and attached in the end, since those prints will not be legible in letter size.